PARAMETER IDENTIFICATION IN PINHOLE CAMERA VISION SYSTEM: AN ENHANCED APPROACH

C.K. Chen[a], M. J. Jang[b] and C. T. Chuang[c]

[a] *Department of Mechanical Engineering, National Cheng Kung University*
[b] *Department of Automation and Control Engineering, Far East College*
[c] *Department of Aeronautics and Astronautics, National Cheng Kung University*
Tainan, Taiwan.

Abstract: The purpose of camera calibration is to reconstruct the world coordinate system using two-dimensional images. A good calibration result depends on identifying the camera parameters successfully. The use of single two-dimensional calibration boards or three-dimensional calibration boxes for camera calibration results in a camera model which is suitable for local operation only. The objective of the present study is to improve the calibration approach in order to identify the system parameters in a more effective and economical manner. The proposed approach improves the use of stereo images in three-dimensional measurement applications.

Keywords: Vision system, Camera calibration, Parameter identification

1. INTRODUCTION

The purpose of camera calibration is to establish the relationship between the coordinates of the three-dimensional world and their projection on an image plane. A successful camera calibration makes it possible to obtain world coordinate values from two-dimensional images. Existing camera calibration techniques can be broadly divided into two approaches, namely the photogrammetry approach and the self-calibration approach. The former requires a calibration pattern whose three-dimensional coordinate values are known. By contrast, the self-calibration approach derives the parameters from camera movement and the corresponding image information. However, self-calibration is not yet a mature technique and is limited by a poor precision and a lack of robustness (Bougnoux, 1998; Sturm, 2002). Camera parameter identification and stereovision system calibration require a calibration pattern in the form of either a two-dimensional calibration board or a three-dimensional calibration box to provide real world information. Different calibration patterns with different feature points have been proposed. For example, Zhang (1999) and Nakano et al. (2002) used single plane patterns. Some patterns have also been reported which provide three-dimensional feature information. However, these patterns can cause certain imperfections as a result of view-direction differences and reflection, and these imperfections can affect the calibration result (Huang and Boufama, 2002). Furthermore, these calibration patterns must be highly precise, and hence their fabrication is relatively costly.

In 1987, Tsai proposed a camera calibration technique for high-accuracy 3D machine vision metrology applications using off-the-shelf TV cameras and lenses. Many other researchers have focused on this issue since that time. Zhang's method proposed in 1999 represents one of the most successful photogrammetry approaches and has been applied in a variety of applications (Ho, 2002). Other related methods have also been reported, including those of Zhang (2002), Frahm and Koch (2003), and Malis (2004).

This paper proposes an enhanced approach for pinhole camera parameter identification based on Zhang's approach. A synthetic calibration box is applied to acquire three-dimensional feature information. The experimental results indicate that the proposed approach provides an effective and economic means of obtaining the camera parameters.

2. CALIBRATION PATTERN

In identifying camera parameters, many researchers employ the single calibration board with two-dimensional features shown in Figure 1(a). However, the results obtained using this board can only be applied locally. In other words, the measurement error arising when using the calibrated camera in a stereovision system is proportional to the distance between the calibration board and the measured object. In order to overcome this limitation, the three-dimensional calibration box (Huang, 2002) shown in Figure 1(b) has been introduced. However, it provides boundary surface information only.

In view of the limitations of the approaches described above, the objective of the present study is to develop a method of acquiring three-dimensional information via a series of movements of a two-dimensional calibration plane, as illustrated in Figure 1(c). The advantages of using this type of calibration pattern can be summarized as follows:

(1). It provides full three-dimensional information.
(2). It can be generated with high precision using a jet printer and can be operated automatically.
(3). In contrast to the single plane approach, it is insensitive to the working range and the working distance between the camera and the calibration pattern.

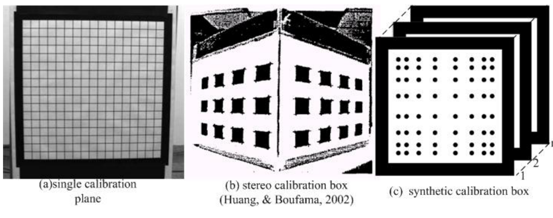

Figure 1. Calibration pattern.

To realize the calibration procedure using the proposed synthetic calibration box it is necessary to modify the algorithm relating to single plane calibration.

2.1 Pinhole camera model

The camera model represents the projective transformation from the three-dimensional world coordinate system, $\widetilde{\mathrm{M}} = [X, Y, Z, 1]^T$, to the two-dimensional image coordinate system, $\widetilde{\mathrm{m}} = [u, v, 1]^T$, and can be described as:

$$\widetilde{\mathrm{m}} = \begin{bmatrix} u \\ v \\ 1 \end{bmatrix} = \lambda \mathbf{A} [\mathbf{r}_1 \quad \mathbf{r}_2 \quad \mathbf{r}_3 \quad \mathbf{t}] \begin{bmatrix} X \\ Y \\ Z \\ 1 \end{bmatrix} \tag{1}$$

where:

$\mathbf{A} = \begin{bmatrix} \alpha & \gamma & u_0 \\ 0 & \beta & v_0 \\ 0 & 0 & 1 \end{bmatrix}$ is the inner camera parameter matrix, $\mathbf{R}=[r_1 \quad r_2 \quad r_3]$, and $\mathbf{t}$ are extrinsic camera parameter matrices relating the camera orientation and position to the world coordinate system. Meanwhile, λ is a scaling factor. To establish the parameter matrices using a single calibration plane, it can be assumed that Z=0, and the calibration algorithm proposed by Zhang (1999) can be applied. However, for the case of $Z \neq 0$, the solution procedure is complex and it is far more challenging to obtain satisfactory results.

2.2 Problem formulation and solution procedure using synthetic calibration box

This section of the paper considers a synthetic calibration box composed of three calibration planes. The obtained results can then be extended to multiple-plane cases. Figure 2 presents a schematic illustration of the experimental set-up used to calibrate the camera using the synthetic calibration box. In practice, the calibration planes may not be precisely parallel, i.e. θ_2 and θ_3 may have small values rather than being zero, as shown in Figure 3. Hence, the camera model for Planes 2 and 3 should be rewritten as:

$$\widetilde{\mathrm{m}} = \begin{bmatrix} u \\ v \\ 1 \end{bmatrix} = \lambda \mathbf{A} [\mathbf{r}_1 \quad \mathbf{r}_2 \quad \mathbf{r}_3 \quad \mathbf{t}] \begin{bmatrix} \cos\theta & 0 & \sin\theta & 0 \\ 0 & 1 & 0 & 0 \\ -\sin\theta & 0 & \cos\theta & 0 \\ 0 & 0 & 0 & 1 \end{bmatrix} \begin{bmatrix} X_p \\ Y_p \\ Z_p \\ 1 \end{bmatrix} \tag{2}$$

where $\theta_i = \theta_2$ or θ_3 , and $\begin{bmatrix} X_p & Y_p & Z_p \end{bmatrix}^T$ represents the ideal feature location in the world coordinate system under the assumption of parallel plane spacing. Therefore, the projection of $\begin{bmatrix} X_p & Y_p & Z_p \end{bmatrix}^T$ to the image coordinates by the camera model with radial distortion can be obtained using the following steps. Initially, let:

$$H' = \mathbf{A}[\mathbf{R}\,|\,\mathbf{T}]\begin{bmatrix} \cos\theta & 0 & \sin\theta & 0 \\ 0 & 1 & 0 & 0 \\ -\sin\theta & 0 & \cos\theta & 0 \\ 0 & 0 & 0 & 1 \end{bmatrix} = \begin{bmatrix} h_{11} & h_{12} & h_{13} & h_{14} \\ h_{21} & h_{22} & h_{23} & h_{24} \\ h_{31} & h_{32} & h_{33} & h_{34} \end{bmatrix} \quad (3)$$

Therefore, the image coordinate values of the object obtained by the ideal pinhole camera model can be described as:

$$u = \frac{h_{11}X_w + h_{12}Y_w + h_{13}Z_w + h_{14}}{h_{31}X_w + h_{32}Y_w + h_{33}Z_w + h_{34}},$$
$$v = \frac{h_{21}X_w + h_{22}Y_w + h_{23}Z_w + h_{24}}{h_{31}X_w + h_{32}Y_w + h_{33}Z_w + h_{34}}. \quad (4)$$

Taking the radial distortion into consideration, the image coordinate values become:

$$\breve{u} = u + (u - u_0)\left[k_1\left(x^2 + y^2\right) + k_2\left(x^2 + y^2\right)^2\right] \quad (5)$$

$$\breve{v} = v + (v - v_0)\left[k_1\left(x^2 + y^2\right) + k_2\left(x^2 + y^2\right)^2\right] \quad (6)$$

Hence, the projection through the camera model is given by:

$$\breve{\mathbf{m}}\left(\mathbf{A}, k_1, k_2, \theta_i, \mathbf{R}_i, \mathbf{t}_i, \mathbf{M}_j\right) = \begin{bmatrix} \breve{u} \\ \breve{v} \\ 1 \end{bmatrix} \quad (7)$$

where i represents the i-th calibration and j represents the j-th ideal feature location in the work coordinate system.

Based on the analysis above, the camera parameters can be obtained using the following procedure:

(1). Based on Zhang's approach (1999), two images from different view directions are employed to obtain the camera parameters using the feature information provided by Plane 1 as the initial values.

(2). Move the calibration plane and obtain the feature information of Planes 2 and 3, respectively. Use the Leverberg-Marquardt optimization algorithm to determine the camera parameters such that the objective function

$$J = \left(\sqrt{\frac{1}{nm}\sum_{i=1}^{n}\sum_{j=1}^{m}\left\| \mathbf{m}_{ij} - \breve{\mathbf{m}}\left(\mathbf{A}, k_1, k_2, \theta_i, \mathbf{R}_i, \mathbf{t}_i, \mathbf{M}_j\right)\right\|}\right)^2 \quad (8)$$

is minimized, where m_{ij} and $\breve{\mathbf{m}}\left(\mathbf{A}, k_1, k_2, \theta_i, \mathbf{R}_i, \mathbf{t}_i, \mathbf{M}_j\right)$ represent the coordinate value obtained by CCD camera and the camera model, respectively.

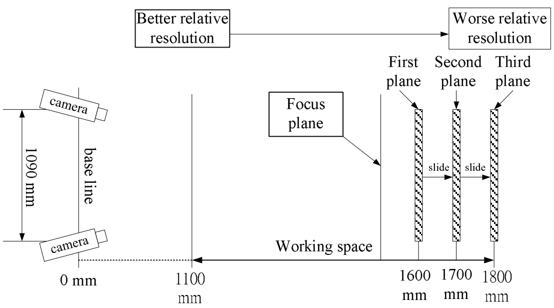

Fig 2. Experimental set-up for camera calibration

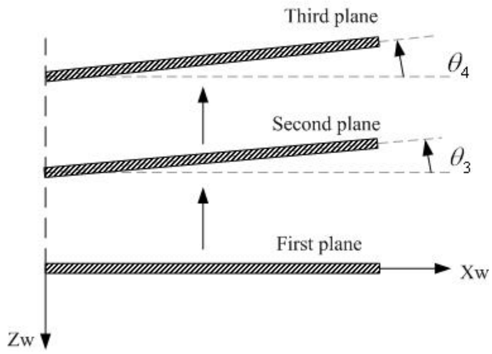

Fig 3. Non-parallel spacing between calibration planes

Consider the calibration plane and stereovision system set-up shown in Figure 4. In this study, each calibration plane provides 36 items of calibration feature information and 4 images are used, i.e. m=36 and n=4 in the objective function given in Eq. (8) above. The CCD cameras (Model SVS084MFCL) are supplied by SVS-Vistek, and have focus lengths of 6mm, imager arrays of 658(H) by 494 (V), and a 7.4 μ m by 7.4 μ m pixel size. According to the supplier, the ideal values of the camera inner parameters, i.e. α and β , are

$$\alpha_{ideal} = \beta_{ideal} = \frac{6000}{7.4} = 810.811\,.$$

The inner parameters of the left and right cameras are obtained using the single calibration plane method and the proposed calibration procedure, respectively. The corresponding results are shown in Table 1. From an inspection of this table, it is clear that the proposed multiple-plane calibration procedure yields superior results.

(a) Left camera (b) Right camera

Fig 4. Calibration pattern and camera system

Table 1. The internal parameters of the cameras

camera	the 1st plane (mm)	the 2nd plane (mm)	the 3rd plane (mm)	α	β	u_0	v_0	k_1	k_2	RMS
Left	1600	X	X	830	831	371	200	-0.24	0.22	0.26
Left	1600	1800	X	817	810	307	201	-0.14	-0.11	0.25
Left	1600	1700	1800	812	806	314	199	-0.09	-0.45	0.23
Right	1600	X	X	882	895	233	210	-0.2	0.25	0.32
Right	1600	1800	X	805	804	354	207	-0.15	-0.11	0.23
Right	1600	1700	1800	808	807	343	205	-0.13	-0.35	0.19

2.3 Reconstruct world coordinate

This study uses Epipolar geometry and fundamental matrix to find out the relationship of corresponding point between left and right cameras (Sonka, 1998). When a point viewed with left and right cameras is assured, the homogeneous transformation relationship between world coordinate and image coordinate can be described as:

$$\begin{bmatrix} u \\ v \\ 1 \end{bmatrix} \equiv \begin{bmatrix} p_{11} & p_{12} & p_{13} & p_{14} \\ p_{21} & p_{22} & p_{23} & p_{24} \\ p_{31} & p_{32} & p_{33} & p_{34} \end{bmatrix} \begin{bmatrix} X_W \\ Y_W \\ Z_W \\ 1 \end{bmatrix} \qquad (9)$$

where

$$u = \frac{p_{11}X_W + p_{12}Y_W + p_{13}Z_W + p_{14}}{p_{31}X_W + p_{32}Y_W + p_{33}Z_W + p_{34}},$$

$$v = \frac{p_{21}X_W + p_{22}Y_W + p_{23}Z_W + p_{24}}{p_{31}X_W + p_{32}Y_W + p_{33}Z_W + p_{34}}.$$

Represent as matrix form:

$$\begin{bmatrix} p_{31}u - p_{11} & p_{32}u - p_{12} & p_{33}u - p_{13} \\ p_{31}v - p_{21} & p_{32}v - p_{22} & p_{33}v - p_{23} \end{bmatrix} \begin{bmatrix} X_W \\ Y_W \\ Z_W \end{bmatrix} = \begin{bmatrix} p_{14} - p_{34}u \\ p_{24} - p_{34}v \end{bmatrix} \qquad (10)$$

Eq. (10) can represent as an over-determined linear equation:

$$\mathbf{A}_{2N\times 3}\mathbf{X}_W = \mathbf{b}_{2N\times 1}, \qquad (11)$$

where N is the number of cameras, and the projective solution of least mean square error is:

$$\mathbf{X}_W = \left(\mathbf{A}^T\mathbf{A}\right)^{-1}\mathbf{A}^T\mathbf{b}, \qquad (12)$$

where the reconstruction of three-dimensional world coordinate will realize.

3. PRECISION ANALYSIS OF IMAGE MEASUREMENT

Although the proposed synthetic calibration box provides precise Z-axis information, the precision of the measurement system is affected by a number of factors.

(1) Parallel parameters of synthetic calibration box

In practice, parallel parameters ($\breve{\mathbf{m}}(\mathbf{A}, k_1, k_2, \theta_i, \mathbf{R}_i, \mathbf{t}_i, \mathbf{M}_j)$) not only influence the accuracy of the camera model, but also increase the measurement precision, as shown in Figure 2, in which the baseline length is 1090mm and the focus plane lies at 1500mm. Figure 5 demonstrates that the parallel parameters reduce the calibration error of the synthetic calibration box containing either two or three calibration planes. The figure also shows that locating the calibration planes at a greater distance (i.e. 1600-1700-1800 or 1600-1800) provides more accurate results than when the planes are positioned closer to the baseline (i.e. 1400-1500-1600 or 1400-1600). Additionally, it is clear that the use of three calibration planes generates a more accurate measurement result than when just two calibration planes are used.

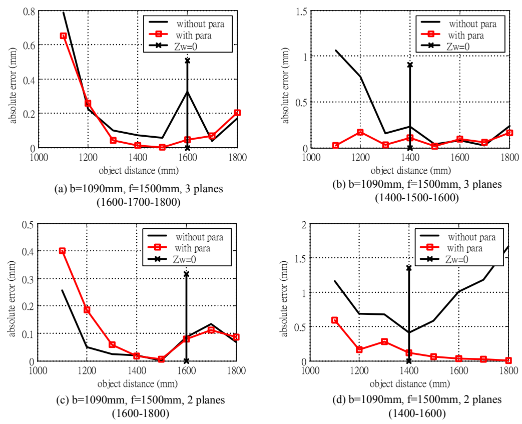

Fig. 5. Calibration error of synthetic calibration box caused by parallel parameters

(2). Focus plane of camera lens

Figure 6 shows that positioning the focus plane at 1100mm enhances the measurement precision. Furthermore, the results indicate that positioning the focus plane in front of the working range ensures a good measurement precision over the entire working range.

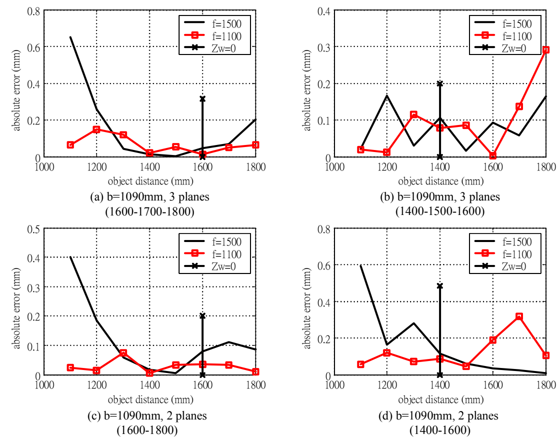

Fig 6. Effect of camera lens focus plane position

(3). Positioning of calibration box

In general, the image resolution decreases as the distance of the calibration box from the camera increases. Figure 7 shows that positioning the calibration box behind the working range will provide a good measurement precision over the complete working range.

(4). Number of constructed planes in synthetic calibration box

Figures 5 and 6 indicate that the degree of measurement precision obtained from two calibration planes is very similar to that obtained from three planes. Figure 8 shows a test object rotated at an angle of -30 degrees by Z-axis. Table 2 shows that the use of three calibration planes ensures a more accurate measurement result when the measured object is rotated at an angle.

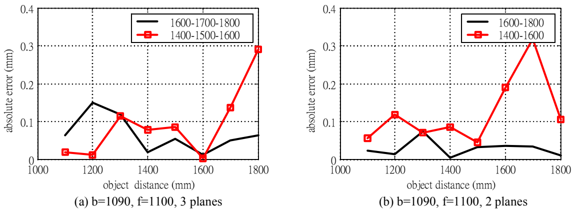

Fig 7 Effect of calibration box position on measurement precision

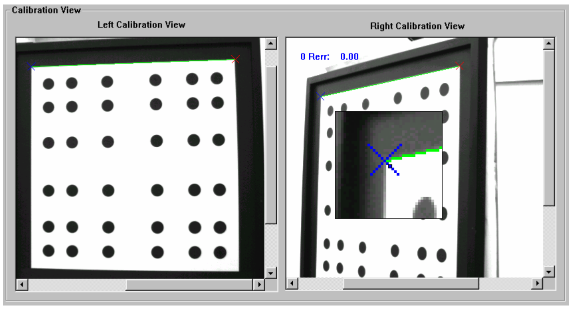

Fig 8. Measurement of test object rotated at angle of -30 degrees

Table 2 Comparison of measurement precision obtained using 2 and 3 calibration planes for inclined test object. (Baseline length 1090mm and measured length 510mm)

(a) Two planes

Measured range (mm)	Measured length (mm)	Error (mm)	STD (mm)	Rotated angle
1200-1400	507.789	-2.211	2.045	-30deg
1400-1600	507.567	-2.433	2.490	-30deg
1600-1800	507.777	-2.223	2.086	-30deg
1200-1400	509.686	-0.314	0.262	30deg
1400-1600	510.216	0.216	0.442	30deg
1600-1800	509.869	-0.131	0.910	30deg
Average	508.817	-1.183		

(b) Three planes

Measured range (mm)	Measured length (mm)	Error (mm)	STD (mm)	Rotated angle
1200-1400	509.404	-0.596	0.565	-30deg
1400-1600	508.727	-1.273	0.895	-30deg
1600-1800	508.720	-1.280	1.701	-30deg
1200-1400	510.053	-0.053	0.442	30deg
1400-1600	509.357	-0.643	0.567	30deg
1600-1800	508.544	-1.456	1.377	30deg
Average	509.134	-0.866		

(5). Length of baseline

Figure 9 shows the effect on the measurement precision of the baseline length. When the baseline is 680mm and the measurement distance exceeds 1300mm, the measurement error increases significantly. Conversely, if the baseline is 1090mm and the measurement distance is 1300mm, the measurement error decreases. Hence, from the relationships $\tan^{-1}(\frac{1300}{545}) \approx 65°$ and $\tan^{-1}(\frac{1300}{340}) \approx 75°$, it can be concluded that the suitable measurement range extends from $65°$ to $75°$.

The measurement conditions specified above are used to measure a cubic box with known dimensions of 260.0mm×159.5mm×68.5mm. Figure 10 shows that the measurement results are 260.348mm × 160.345mm × 69.188mm. In other words, the measurement errors are less than 1mm in each dimension. This result confirms that the measurement method proposed in this paper is capable of providing a high degree of precision when the test object is positioned within the working range.

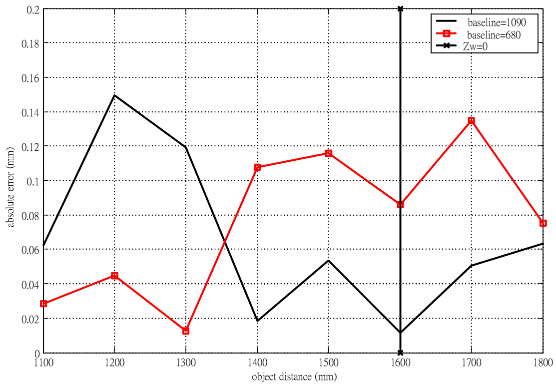

Fig 9. Effect of baseline length on measurement precision (*f*=1100, 3 planes)

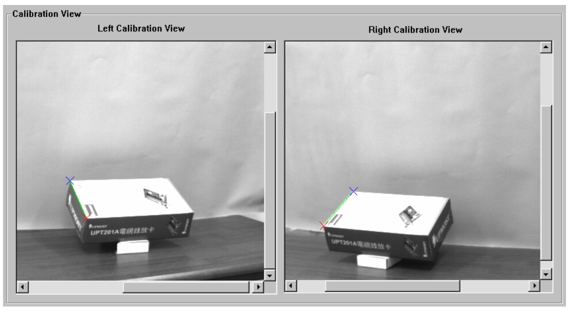

Fig 10. Three-dimensional measurement of cubic box

4. CONCLUSION

This paper has proposed the use of a synthetic calibration box to identify the internal parameters of a pinhole camera. The proposed calibration procedure provides superior results compared to those generated using the conventional single plane calibration method. The current measurement error analysis has shown that the measurement accuracy is enhanced under the following conditions: (1) three calibration planes are used, (2) the calibration box is positioned behind the working range, and (3) the focus plane is located in front of the working range. The results presented in this study can be applied to realize a low-cost 3D visual measurement system with improved measurement performance.

ACKNOWLEDGMENT

The current authors gratefully acknowledge the support provided to this study by the National Science Council of Taiwan under Grant No. NSC92-2212-E-006-037.

REFERENCES

Bougnoux, S. (1998). From projective to Euclidean space under any practical situation, a criticism of self-calibration. *Proceedings of the 6th International Conference on Computer Vision*, 790-796.

Frahm, J. M. and Koch, R. (2003). Camera calibration with known rotation. *Proceedings of the Ninth IEEE International Conference on Computer Vision*, 1418-1425.

Ho, I. D., (2002), Three dimensional target trajectory estimation and interception by servo technology. *MSc Dissertation, National Cheng Kung University*, Tainan, Taiwan.

Huang, Z., and Boufama, B. (2002). A semi-automatic camera calibration method for augmented reality. *2002 IEEE International Conference on Systems, Man and Cybernetics*, Volume: 4 , 6-9 Oct. 2002 Pages:6 pp. vol.4, TP1H6.

Malis, E. (2004). Visual servoing invariant to changes in camera-intrinsic parameters. *IEEE Transaction on Robotics and Automation*, **20** (1), 72-81.

Nakano, K. Okutomi, M. and Kasegawa, Y. (2002). Camera calibration with precise extraction of feature points using projective transformation. *Proceedings of the 2002 IEEE International Conference on Robotics and Automation,* 2532-2538.

Sturm, P. (2002). Critical motion sequences for the self-calibration cameras and stereo systems with variable focal length. *Image Vis. Comput*, **20**, no. 5-6, 415-426

Sonka, M., Hlavac, V., and Boyle, R. (1998). *Image processing, analysis, and machine vision*. California: PWS.

Tsai, R. (1987). A versatile camera calibration technique for high-accuracy 3D machine vision metrology using off-the-shelf TV cameras and lenses. *IEEE Journal of Robotics and Automation*. **3** (4), 323-344.

Zhang, Z. (1999). A flexible new technique for camera calibration. *Technical Report MSR-TR-98-71*, Microsoft Research.

Zhang, Z. (2002). Camera calibration with one-dimensional objects. *Technical Report MSR-TR-2001-120*, Microsoft Research.